

## Synthesis, Structural Characterization, Catalytic Properties, and Theoretical Study of Compounds Containing an Al–O–M (M = Ti, Hf) Core

Prabhuodeyara M. Gurubasavaraj, Swadhin K. Mandal, Herbert W. Roesky,\* Rainer B. Oswald, Aritra Pal, and Mathias Noltemeyer

Institut für Anorganische Chemie der Georg-August-Universität Göttingen, Tammannstrasse 4, 37077 Göttingen, Germany

Received March 30, 2006

Two single oxygen-bridged heterobimetallic oxides of Al(III) with group 4 metals (Ti, Hf) have been prepared. The reaction of  $\text{LAlMeOH}$  (**1**) [ $\text{L} = \text{CH}(\text{N}(\text{Ar})(\text{CMe})_2)$ ,  $\text{Ar} = 2,6\text{-}i\text{Pr}_2\text{C}_6\text{H}_3$ ] with dimethylmetallocenes of Ti and Hf in toluene (80 °C) and ether (room temperature), respectively, resulted in the formation of  $\text{LAl}(\text{Me})(\mu\text{-O})\text{M}(\text{Me})\text{Cp}_2$  [ $\text{M} = \text{Ti}$  (**2**),  $\text{Hf}$  (**3**)] in moderate to good yield. Compounds **2** and **3** were characterized by elemental analysis, IR, NMR ( $^1\text{H}$  and  $^{13}\text{C}$ ), EI-MS, and single-crystal X-ray structural analysis. Furthermore, compound **2** showed good catalytic activity in ethylene and styrene homopolymerization, while compound **3** is less active in ethylene polymerization. The styrene polymerization yields atactic polystyrene.

### Introduction

The synthesis and characterization of heterobimetallic oxides, which are used as polyfunctional catalysts and precursors for the preparation of bi- and polymetallic heterogeneous catalysts, have been the topic of various academic and industrial studies<sup>1</sup> since the discovery of catalytic olefin polymerization by Ziegler and Natta. These heterogeneous catalysts have complicated structural features and are insoluble in solvents advantageous for polymerization reactions. Investigations by Sinn and Kaminsky<sup>2</sup> reveal that soluble metallocene catalysts in combination with methylalumoxane (MAO) achieve extremely high activities in the polymerization of olefins leading to new developments in this field. These investigations are accompanied by an increased understanding of the factors that are important for stabilizing polymerization-active metal centers and controlling their activity and selectivity.<sup>3</sup> The design and synthesis of new transition metal precursors and main group organo-

metallic cocatalysts is a very important subject which can provide high catalytic activity with a low cocatalyst to catalyst precursor ratio, and this allows unprecedented control over the polymer microstructure generating new polymers with improved properties. Well-defined single-site metallocene catalysts are slowly replacing the conventional heterogeneous Ziegler–Natta catalysts.

Recent work from our laboratory described the preparation of heterobimetallic oxides of aluminum with zirconium which showed high catalytic activity in the olefin polymerization reaction.<sup>4</sup> Instead of routine long-chain and three-dimensional cage compounds, we isolated unprecedented aluminum dihydroxide-containing terminal OH groups  $\text{LAl}(\text{OH})_2$  [ $\text{L} = \text{CH}(\text{N}(\text{Ar})(\text{CMe})_2)$ ,  $\text{Ar} = 2,6\text{-}i\text{Pr}_2\text{C}_6\text{H}_3$ ] by treatment of  $\text{LAlI}_2$  with KOH containing 10–15%  $\text{H}_2\text{O}$  and KH in liquid ammonia.<sup>5</sup> Then, we reported an improved route to  $\text{LAl}(\text{OH})_2$  using a strong nucleophilic reagent N-heterocyclic carbene as a HCl acceptor for the reaction of  $\text{LAlCl}_2$  and stoichiometric amounts of water.<sup>6</sup> In the course of the synthesis of  $\text{LAlMe}(\text{OH})$  from  $\text{LAlMeCl}$ , a stepwise process

\* To whom correspondence should be addressed. E-mail: hroesky@gwdg.de.

- (1) (a) Copéret, C.; Chabanas, M.; Saint-Arroman, R. P.; Basset, J.-M. *Angew. Chem.* **2003**, *115*, 164–191.; *Angew. Chem., Int. Ed.* **2003**, *42*, 156–181. (b) Roesky, H. W.; Haiduc, I.; Hosmane, N. S. *Chem. Rev.* **2003**, *103*, 2579–2595.
- (2) Andresen, A.; Cordes, H.-G.; Herwig, J.; Kaminsky, W.; Merck, A.; Mottweiler, R.; Pein, J.; Sinn, H.; Vollmer, H.-J. *Angew. Chem.* **1976**, *88*, 689–690; *Angew. Chem., Int. Ed.* **1976**, *15*, 630–632.
- (3) Chen, E. Y.-X.; Marks, T. J. *Chem. Rev.* **2000**, *100*, 1391–1434.

- (4) Bai, G.; Singh, S.; Roesky, H. W.; Noltemeyer, M.; Schmidt, H.-G. *J. Am. Chem. Soc.* **2005**, *127*, 3449–3455.
- (5) Bai, G.; Peng, Y.; Roesky, H. W.; Li, J.; Schmidt, H.-G.; Noltemeyer, M. *Angew. Chem.* **2003**, *115*, 1164–1167; *Angew. Chem., Int. Ed.* **2003**, *42*, 1132–1135.
- (6) Jancik, V.; Pineda, L. W.; Pinkas, J.; Roesky, H. W.; Neculai, D.; Neculai, A. M.; Herbst-Irmer, R. *Angew. Chem.* **2004**, *116*, 2194–2197; *Angew. Chem., Int. Ed.* **2004**, *43*, 2142–2145.

was followed with 1 equiv of water. Recently, we became interested in the preparation of heterodinuclear complexes of aluminum with early transition metals and the use of such systems as catalysts for the polymerization of olefins.<sup>4</sup>

Herein, we report the reaction of LAlMeOH (**1**) [L = CH-(N(Ar)(CMe))<sub>2</sub>, Ar = 2,6-*i*Pr<sub>2</sub>C<sub>6</sub>H<sub>3</sub>] with methylated metallocene derivatives of group 4 metals (Ti, Hf) leading to the isolation and characterization of discrete new  $\mu$ -oxo heterobimetallic systems. Compounds **2** and **3** have been tested as catalysts for the polymerization of olefins. Compound **2** showed high catalytic activity with a low MAO to catalyst ratio in ethylene and styrene polymerization, whereas compound **3** showed low activity in the polymerization of ethylene.

## Experimental Section

**General Comments.** All experimental manipulations were carried out under an atmosphere of dry nitrogen using standard Schlenk techniques. The samples for spectral measurements were prepared in a glovebox. The solvents were purified according to conventional procedures and were freshly distilled prior to use. Titanocene and hafnocene dichlorides were purchased from Aldrich and Fluka, respectively, and were used as received. Cp<sub>2</sub>TiMe<sub>2</sub> and Cp<sub>2</sub>HfMe<sub>2</sub> were prepared by the procedure which was published elsewhere.<sup>7</sup> NMR spectra were recorded on a Bruker Avance 500 instrument, and the chemical shifts are reported with reference to tetramethylsilane (TMS). IR spectra were recorded on a Bio-Rad Digilab FTS-7 spectrometer. Mass spectra were obtained on a Finnigan MAT 8230 spectrometer by the EI technique. Melting points were obtained in sealed capillaries on a Büchi B 540 instrument. Elemental analyses were performed at the Analytical Laboratory of the Institute of Inorganic Chemistry at Göttingen, Germany.

**Preparation of LAl(Me)( $\mu$ -O)Ti(Me)Cp<sub>2</sub> (**2**).** A solution of freshly prepared Cp<sub>2</sub>TiMe<sub>2</sub> (0.21 g, 1.01 mmol) in toluene (20 mL) was added via cannula to a solution of LAlMeOH (**1**) [L = CH-(N(Ar)(CMe))<sub>2</sub>, Ar = 2,6-*i*Pr<sub>2</sub>C<sub>6</sub>H<sub>3</sub>] (0.48 g, 1.01 mmol) in toluene (20 mL) at ambient temperature. (NOTE: Care must be taken because Cp<sub>2</sub>TiMe<sub>2</sub> is photosensitive.) The reaction mixture was heated to 80 °C for 18 h under stirring. The yellow precipitate formed was filtered off, washed with *n*-hexane, and dried in vacuum. Yield: 0.41 g (61%). mp (dec): 250 °C. <sup>1</sup>H NMR (500.13 MHz, C<sub>6</sub>D<sub>6</sub>, 25 °C, TMS):  $\delta$  7.13–7.24 (m, 6H, *m*-, *p*-Ar-H), 5.30 (s, 10H, C<sub>5</sub>H<sub>5</sub>), 4.90 (s, 1H,  $\gamma$ -CH), 3.10 (sept, 4H, <sup>3</sup>J<sub>H-H</sub> = 6.8 Hz, CH(CH<sub>3</sub>)<sub>2</sub>), 1.68 (s, 6H, CH<sub>3</sub>), 1.40 (d, 12H, <sup>3</sup>J<sub>H-H</sub> = 6.8 Hz, CH(CH<sub>3</sub>)<sub>2</sub>), 1.31 (d, 12H, <sup>3</sup>J<sub>H-H</sub> = 6.8 Hz, CH(CH<sub>3</sub>)<sub>2</sub>), -0.18 (s, 3H, Ti-CH<sub>3</sub>), -0.91 (s, 3H, Al-CH<sub>3</sub>). <sup>13</sup>C NMR (125.75 MHz, C<sub>6</sub>D<sub>6</sub>, 25 °C, TMS):  $\delta$  165.4(CN), 145.3, 144.8, 142.8, 128.6, 125.9, 125.2 (*i*-, *o*-, *m*-, *p*-Ar), 111.3 (C<sub>5</sub>H<sub>5</sub>), 97.0 ( $\gamma$ -CH), 27.9 (Ti-CH<sub>3</sub>), 26.5 (Al-CH<sub>3</sub>). EI-MS (70 eV) [*m/e* (%): 653 (100) [*M*<sup>+</sup> - Me], 638 (48) [*M*<sup>+</sup> - 2Me], 202 (26) [DippNCMe]<sup>+</sup>. Anal. Calcd for C<sub>41</sub>H<sub>57</sub>AlN<sub>2</sub>O<sub>2</sub>Ti (*M*<sub>r</sub> = 668.75): C, 73.64; H, 8.59; N, 4.19. Found: C, 72.28; H, 8.47; N, 4.17.

**Preparation of LAl(Me)( $\mu$ -O)Hf(Me)Cp<sub>2</sub> (**3**).** Freshly sublimed Cp<sub>2</sub>HfMe<sub>2</sub> (0.34 g, 1 mmol), dissolved in ether (20 mL), was transferred using a cannula to a flask charged with **1** (0.48 g, 1 mmol) in diethyl ether (30 mL) at -30 °C. The reaction mixture

**Table 1.** Crystal Data and Structure Refinement for Compounds **2** and **3**

	<b>2</b>	<b>3</b>
formula	C <sub>41</sub> H <sub>57</sub> AlN <sub>2</sub> O <sub>2</sub> Ti	C <sub>41</sub> H <sub>57</sub> AlHfN <sub>2</sub> O
fw	668.77	799.36
color	yellow	colorless
temp (K)	100(2)	133(2)
cryst syst	triclinic	triclinic
space group	<i>P</i> $\bar{1}$	<i>P</i> $\bar{1}$
<i>a</i> (Å)	9.572(2)	9.921(2)
<i>b</i> (Å)	10.422(2)	10.276(2)
<i>c</i> (Å)	20.060(3)	19.616(3)
$\alpha$ (deg)	90.13(2)	88.28(2)
$\beta$ (deg)	90.55(2)	87.17(2)
$\gamma$ (deg)	114.14(2)	68.47(2)
<i>V</i> (Å <sup>3</sup> )	1886.0(6)	1857.9(6)
<i>Z</i>	2	2
$\rho_{\text{calcd}}$ (g cm <sup>-3</sup> )	1.216	1.429
$\mu$ (mm <sup>-1</sup> )	2.464	2.864
<i>F</i> (000)	720	820
$\theta$ range (deg)	4.41–58.99	2.08–24.81
index ranges	-10 $\leq h \leq$ 10 -11 $\leq k \leq$ 11 -22 $\leq l \leq$ 20	-11 $\leq h \leq$ 11 -12 $\leq k \leq$ 12 -23 $\leq l \leq$ 23
data/restraints/params	5056/704/531	6373/1/431
refinement method	full-matrix least-squares on <i>F</i> <sup>2</sup>	full-matrix least-squares on <i>F</i> <sup>2</sup>
GOF on <i>F</i> <sup>2</sup>	1.195	1.028
R1, wR2 ( <i>I</i> > 2 $\sigma$ ( <i>I</i> ))	0.0603, 0.1205	0.0178, 0.0369
R1, wR2 (all data)	0.0760, 0.1265	0.0221, 0.0375
largest diff peak, hole (e Å <sup>-3</sup> )	0.301/-0.368	0.370/-0.412

was slowly warmed to ambient temperature and stirred for 18 h. The precipitate was filtered, washed with *n*-hexane, and dried in vacuum. Yield: 0.54 g (67.4%). mp (dec): 391 °C. <sup>1</sup>H NMR (500.13 MHz, C<sub>6</sub>D<sub>6</sub>, 25 °C, TMS):  $\delta$  7.13–7.24 (m, 6H, *m*-, *p*-Ar-H), 5.40 (s, 10H, C<sub>5</sub>H<sub>5</sub>), 4.80 (s, 1H,  $\gamma$ -CH), 3.30 (sept, 4H, <sup>3</sup>J<sub>H-H</sub> = 6.8 Hz, CH(CH<sub>3</sub>)<sub>2</sub>), 1.76 (s, 6H, CH<sub>3</sub>), 1.61 (d, 12H, <sup>3</sup>J<sub>H-H</sub> = 6.8 Hz, CH(CH<sub>3</sub>)<sub>2</sub>), 1.42 (d, 12H, <sup>3</sup>J<sub>H-H</sub> = 6.8 Hz, CH(CH<sub>3</sub>)<sub>2</sub>), 0.08 (s, 3H, Hf-CH<sub>3</sub>), -0.27 (s, 3H, Al-CH<sub>3</sub>). <sup>13</sup>C NMR (125.75 MHz, C<sub>6</sub>D<sub>6</sub>, 25 °C, TMS):  $\delta$  168.3 (CN), 149.5, 146.6, 144.7, 132.4, 135.5, 137.9 (*i*-, *o*-, *m*-, *p*-Ar), 116.3 (C<sub>5</sub>H<sub>5</sub>), 102.0 ( $\gamma$ -CH), 52.9 (Hf-CH<sub>3</sub>), 32.5 (Al-CH<sub>3</sub>). EI-MS (70 eV) [*m/e* (%): 785 (100) [*M*<sup>+</sup> - Me], 770 (8) [*M*<sup>+</sup> - 2Me], 202 (26) [DippNCMe]<sup>+</sup>. Anal. Calcd for C<sub>41</sub>H<sub>57</sub>AlHfN<sub>2</sub>O (*M*<sub>r</sub> = 799.36): C, 61.60; H, 7.19; N, 3.50. Found: C, 59.08; H, 6.85; N, 3.32.

**X-ray Structure Determination of **2** and **3**.** Data for the structure of **2** were collected on a Bruker three-circle diffractometer equipped with a SMART 6000 CCD detector. The data for the structure of **3** were collected on a STOE IPDS II diffractometer. Intensity measurements were performed on a rapidly cooled crystal. The structures were solved by direct methods (SHELXS-97)<sup>8</sup> and refined with all data by full-matrix least-squares on *F*<sup>2</sup>.<sup>9</sup> The hydrogen atoms on the C-H bonds were placed in idealized positions and refined isotropically with a riding model, whereas the non-hydrogen atoms were refined anisotropically. Crystals of **2** were pseudomerohedrally twinned. The fractional contribution of the minor domain refined to 0.061(1). The Cp groups and the Me group attached to the titanium were disordered. They were refined with distance restraints and restraints for the anisotropic displacement parameters. Crystal data are shown in Table 1.

(8) Sheldrick, G. M. SHELXS-97, Program for Structure Solution. *Acta Crystallogr., Sect. A* **1990**, *46*, 467–473.

(9) Sheldrick, G. M. SHELXL-97, Program for Crystal Structure Refinement; University of Göttingen: Göttingen, Germany, 1997.

(7) Samuel, E.; Rausch, M. D. *J. Am. Chem. Soc.* **1973**, *95*, 6263–6267.  
(b) Alt, H. G.; DiSanzo, F. D.; Rausch, M. D.; Uden, P. C. *J. Organomet. Chem.* **1976**, *107*, 257–263.

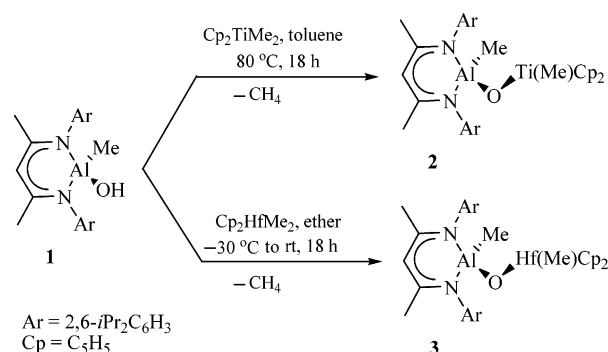
**Polymerization of Ethylene and Styrene.** On a high-vacuum line ( $10^{-5}$  Torr), polymerizations were carried out in a 200 mL autoclave (Büchi). In a typical experiment, 100 mL of dry toluene (from Na/K) was vacuum transferred into the polymerization flask and saturated with 1.0 atm of rigorously purified ethylene (for ethylene homopolymerization) or with argon in the presence of 10 mL of dry styrene (from  $\text{CaH}_2$ ) (for styrene homopolymerization). The catalyst (see Tables 3 and 4) was placed in the Schlenk flask, and the appropriate MAO (1.6 M in toluene) was added. The mixture was stirred for 20 min at room temperature to activate the catalyst. The catalyst solution was then quickly injected into the rapidly stirred autoclave using a gastight syringe. After a measured time interval, the polymerization was quenched by the addition of 5 mL of methanol, and the reaction mixture was then poured into 800 mL of methanol. The polymer was allowed to fully precipitate overnight, and then it was collected by filtration, washed with fresh methanol, and dried.

**Computational Details.** The calculations were performed at a well-established DFT level of theory using the B3LYP-functional<sup>10–11</sup> as implemented in the Gaussian program package<sup>12</sup> and the basis sets LANL2DZ<sup>13</sup> for Ti and 6-31G<sup>14–15</sup> with additional double-diffuse functions for the remaining atoms. In the first step, the compound was fully optimized to its equilibrium structure. The analysis of the resulting electronic wavefunction for this structure was then used to obtain the shape of the molecular orbitals and to analyze the bonding situation by means of a NBO analysis.<sup>16–18</sup>

## Results and Discussions

Using the advantage of the oxophilicity of group 4 metals and the Brønsted acidic character of the proton of the Al(O–H) moiety, we isolated compounds **2** and **3** by treatment of equivalent amounts of  $\text{LAlMeOH}$  (**1**) [ $\text{L} = \text{CH}(\text{N}(\text{Ar})-\text{CMe})_2$ ,  $\text{Ar} = 2,6\text{-}i\text{Pr}_2\text{C}_6\text{H}_3$ ] and  $\text{Cp}_2\text{MMe}_2$  ( $\text{M} = \text{Ti}, \text{Hf}$ ).<sup>7</sup> Reaction of **1** with  $\text{Cp}_2\text{TiMe}_2$  at 80 °C led to the intermolecular elimination of methane and the formation of the  $\mu\text{-O}$ -bridged heterodinuclear complex [ $\text{LAlMe}(\mu\text{-O})\text{Ti}(\text{Me})\text{Cp}_2$ ] (**2**, Scheme 1) in moderate yield (61%). Similarly, treatment of **1** with a stoichiometric amount of  $\text{Cp}_2\text{HfMe}_2$

Scheme 1



in ether in the range from  $-30$  °C to ambient temperature results in the formation of the  $\mu\text{-O}$ -bridged heterodinuclear compound [ $\text{LAlMe}(\mu\text{-O})\text{Hf}(\text{Me})\text{Cp}_2$ ] (**3**, Scheme 1) in good yield (67%).

Compounds **2** and **3** are not soluble in toluene, hexane, and ether, but they are soluble in hot toluene and are characterized by analytical, spectroscopic, and single-crystal X-ray diffraction studies. The IR spectra of **2** and **3** show no OH absorptions in the range from 3000 to 3600  $\text{cm}^{-1}$ , confirming the completion of the reaction by deprotonation. Compound **2** is a yellow crystalline solid that melts at 250 °C, while **3** is a colorless crystalline solid that melts at 391 °C. Decomposition was observed at the melting points of **2** and **3**. Unlike  $\text{Cp}_2\text{TiMe}_2$ , complex **2** is thermally stable and not photosensitive. Compound **2** can be stored for a period of time at room temperature in the absence of air and moisture. The mass spectral data for both **2** and **3** are in agreement with the assigned structures. Neither of them exhibits a molecular ion. Compound **2** shows the base peak at  $m/e$  638 corresponding to  $[\text{M} - 2\text{Me}]^+$ . The next most-intense peak for compound **2** is observed at  $m/e$  653 which can be assigned to  $[\text{M} - \text{Me}]^+$ . The base peak for compound **3** is observed at  $m/e$  785 representing  $[\text{M} - \text{Me}]^+$ . The next most-intense peak at  $m/e$  770 shows the loss of another methyl group corresponding to  $[\text{M} - 2\text{Me}]^+$ . Both compounds **2** and **3** exhibit ions at  $m/e$  202 which can be assigned to  $[\text{DippNCMe}]^+$ .<sup>19</sup> The  $^1\text{H}$  NMR spectrum of **2** exhibits two resonances ( $-0.91$  and  $-0.18$  ppm) which can be attributed to the Me protons of the AlMe and TiMe groups, respectively, whereas the respective AlMe and HfMe groups in compound **3** resonate at  $-0.27$  and 0.08 ppm. The characteristic Cp protons for **2** and **3** appear as singlets (5.3 and 5.4 ppm). In addition, a set of resonances assignable to the isopropyl and methyl protons associated with the  $\beta$ -diketiminate ligand is found in the range between 1.76 and 1.01 ppm, and the absence of the OH proton resonance features both **2** and **3**. The  $^{27}\text{Al}$  NMR is silent because of the quadruple moment of aluminum.

**Molecular Structure Description of 2 and 3.** The yellow single crystals of **2** and the colorless single crystals of **3** were obtained from cooling their hot toluene solutions and were unambiguously analyzed by X-ray diffraction studies (Figures 1 and 2). The crystallographic data for the structural analysis

- (10) Lee, C.; Yang, W.; Parr, R. G. *Phys. Rev. B* **1988**, *37*, 785–78.
- (11) Miehlich, B.; Savin, A.; Stoll, H.; Preuss, H. *Chem. Phys. Lett.* **1989**, *157*, 200–206.
- (12) Frisch, M. J.; Trucks, G. W.; Schlegel, H. B.; Scuseria, G. E.; Robb, M. A.; Cheeseman, J. R.; Montgomery, J. A.; Vreven, T., Jr.; Kudin, K. N.; Burant, J. C.; Millam, J. M.; Iyengar, S. S.; Tomasi, J.; Barone, V.; Mennucci, B.; Cossi, M.; Scalmani, G.; Rega, N.; Petersson, G. A.; Nakatsuji, H.; Hada, M.; Ehara, M.; Toyota, K.; Fukuda, R.; Hasegawa, J.; Ishida, M.; Nakajima, T.; Honda, Y.; Kitao, O.; Nakai, H.; Klene, M.; Li, X.; Knox, J. E.; Hratchian, H. P.; Cross, J. B.; Bakken, V.; Adamo, C.; Jaramillo, J.; Gomperts, R.; Stratmann, R. E.; Yazyev, O.; Austin, A. J.; Cammi, R.; Pomelli, C.; Ochterski, J. W.; Ayala, P. Y.; Morokuma, K.; Voth, G. A.; Salvador, P.; Dannenberg, J. J.; Zakrzewski, V. G.; Dapprich, S.; Daniels, A. D.; Strain, M. C.; Farkas, O.; Malick, D. K.; Rabuck, A. D.; Raghavachari, K.; Foresman, J. B.; Ortiz, J. V.; Cui, Q.; Baboul, A. G.; Clifford, S.; Cioslowski, J.; Stefanov, B. B.; Liu, G.; Liashenko, A.; Piskorz, P.; Komaromi, I.; Martin, R. L.; Fox, D. J.; Keith, T.; Al-Laham, M. A.; Peng, C. Y.; Nanayakkara, A.; Challacombe, M.; Gill, P. M. W.; Johnson, B.; Chen, W.; Wong, M. W.; Gonzalez, C.; Pople, J. A. *Gaussian 03*, revision C.02; Gaussian, Inc., Wallingford CT, 2004.
- (13) Hay, P. J.; Wadt, W. R. *J. Chem. Phys.* **1985**, *82*, 270–283.
- (14) Petersson, G. A.; Al-Laham, M. A. *J. Chem. Phys.* **1991**, *94*, 6081–6090.
- (15) Petersson, G. A.; Bennett, A.; Tensfeldt, T. G.; Al-Laham, M. A.; Shirley, W. A.; Mantzaris, J. *J. Chem. Phys.* **1988**, *89*, 2193–2218.
- (16) Foster, J. P.; Weinhold, F. *J. Am. Chem. Soc.* **1980**, *102*, 7211–7218.
- (17) Reed, A. E.; Weinhold, F. *J. Chem. Phys.* **1985**, *83*, 1736–1740.
- (18) Reed, A. E.; Curtiss, L. A.; Weinhold, F. *Chem. Rev.* **1988**, *88*, 899–926.

- (19) Prust, J.; Most, K.; Müller, I.; Alexopoulos, E.; Stasch, A.; Usón, I.; Roesky, H. W. *Z. Anorg. Allg. Chem.* **2001**, *627*, 2032–2037.

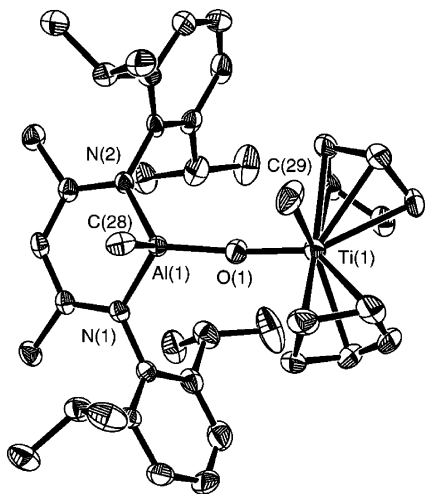


**Figure 1.** Molecular structure of **2** in the crystal (50% probability ellipsoids); hydrogen atoms are omitted for clarity.

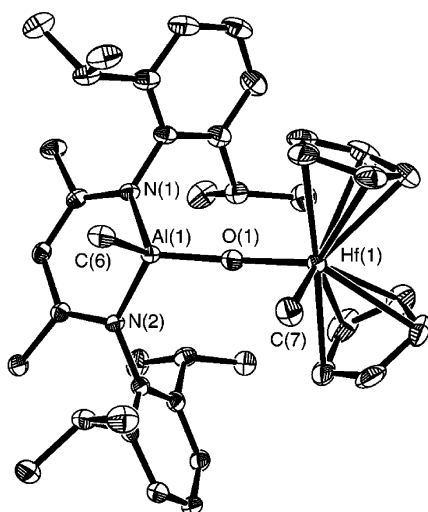


**Figure 2.** Molecular structure of **3** in the crystal (50% probability ellipsoids); hydrogen atoms are omitted for clarity.

of compounds **2** and **3** are given in Table 1. The important bond parameters are listed in Table 2.

Compounds **2** and **3** crystallize in the triclinic space group  $P\bar{1}$ . Both compounds show the aluminum atom bonded through an oxygen atom to titanium and hafnium, respectively, and contain a bent Al–O–M (M = Ti, Hf) core. The aluminum atom exhibits a highly distorted tetrahedral geometry with two nitrogen atoms of the  $\beta$ -diketiminato ligand, a methyl group, and one ( $\mu$ -O) unit. The titanium and hafnium exhibit tetrahedral geometry and their coordination spheres are completed by two Cp ligands and one methyl group around each metal atom. The Me groups on Al and Ti in **2** and **3** are bent out of the Al–O–M (M = Ti, Hf) plane in a cis configuration.

The Al–( $\mu$ -O) bond length (1.715(3) Å) in **2** is in good agreement with LMeAl–( $\mu$ -O)–ZrRCp<sub>2</sub> (L = CH(N(Ar)(CMe))<sub>2</sub>, Ar = 2,6-*i*Pr<sub>2</sub>C<sub>6</sub>H<sub>3</sub>, R = Me, Cl) (av 1.721 Å)<sup>4</sup> but is longer than those found in compounds [(Me<sub>3</sub>-Si)<sub>2</sub>HC]<sub>2</sub>Al]<sub>2</sub>( $\mu$ -O) (1.687(4) Å)<sup>20</sup> and [HC{(CMe)-(NMe)}<sub>2</sub>AlCl]<sub>2</sub>( $\mu$ -O) (1.677(6) Å).<sup>21</sup> The Al–( $\mu$ -O)–Ti angle (151.7(2)°) in **2** is smaller than the Al–( $\mu$ -O)–Hf (158.4-

**Table 2.** Selected Bond Distances (Å) and Angles (deg) for Compounds **2** and **3**<sup>a</sup>

compound <b>2</b>			
Ti(1)–O(1)	1.808(3)	Ti(1)–C(29)	2.239(9)
Al(1)–N(1)	1.926(3)	Al(1)–O(1)	1.715(3)
Al(1)–N(2)	1.919(3)	Al(1)–C(28)	1.958(4)
X <sub>cp1</sub> –Ti(1)	2.134	X <sub>cp2</sub> –Ti(1)	2.081
N(2)–Al(1)–N(1)	95.7(1)	O(1)–Al(1)–N(2)	113.9(2)
O(1)–Al(1)–N(1)	111.0(2)	O(1)–Al(1)–C(28)	115.2(2)
N(2)–Al(1)–C(28)	110.9(2)	N(1)–Al(1)–C(28)	108.2(2)
Al(1)–O(1)–Ti(1)	151.7(2)	X <sub>cp1</sub> –Ti(1)–X <sub>cp2</sub>	130.6
X <sub>cp1</sub> –Ti(1)–C(29)	100.6	X <sub>cp2</sub> –Ti(1)–C(29)	99.7
O(1)–Ti(1)–C(29)	95.6(5)	X <sub>cp2</sub> –Ti(1)–O(1)	110.4
X <sub>cp1</sub> –Ti(1)–O(1)	111.8		
compound <b>3</b>			
Hf(1)–O(1)	1.919(2)	Hf(1)–C(7)	2.281(2)
Al(1)–N(1)	1.932(2)	Al(1)–O(1)	1.71(2)
Al(1)–N(2)	1.913(2)	Al(1)–C(6)	1.965(2)
X <sub>cp1</sub> –Hf	2.249	X <sub>cp2</sub> –Hf	2.224
N(2)–Al(1)–N(1)	95.1(1)	O(1)–Al(1)–N(2)	114.0(1)
O(1)–Al(1)–N(1)	111.6(1)	O(1)–Al(1)–C(6)	113.3(1)
N(2)–Al(1)–C(6)	111.7(1)	N(1)–Al(1)–C(6)	109.8
Al(1)–O(1)–Hf(1)	158.4(1)	X <sub>cp1</sub> –Hf–X <sub>cp2</sub>	129.8
X <sub>cp1</sub> –Hf–C(7)	102.3	X <sub>cp2</sub> –Hf–C(7)	103.3
O(1)–Hf–C(7)	99.5(1)	X <sub>cp2</sub> –Hf–O(1)	107.3
X <sub>cp1</sub> –Hf–O(1)	110.0		

<sup>a</sup> X<sub>Cp</sub> = centroid of the Cp ring.

(1)°) angle in **3**, and the corresponding Al–( $\mu$ -O)–Zr bond angle in LMeAl–( $\mu$ -O)–ZrRCp<sub>2</sub> (L = CH(N(Ar)(CMe))<sub>2</sub>, Ar = 2,6-*i*Pr<sub>2</sub>C<sub>6</sub>H<sub>3</sub>, R = Me, Cl) (158.2(1)°).<sup>4</sup> This can probably be attributed to the increasing atomic radii from Ti to Zr causing gradual opening of the Al–O–M (M = Ti, Hf) bond angle and to the bulkiness of the ligands surrounding the metal centers. However, the Al–( $\mu$ -O)–M (M = Ti, Hf) angles in **2** and **3** are significantly less opened than those of homobimetallic M–( $\mu$ -O)–M (M = Zr, Hf) in (Cp<sub>2</sub>ZrMe)<sub>2</sub>( $\mu$ -O) (174.1(3)°)<sup>22</sup> and (Cp<sub>2</sub>HfMe)<sub>2</sub>( $\mu$ -O) (173.9(3)°).<sup>23</sup> The Al–Me bond length in compound **2** (1.958(4) Å) is similar to that of LAlMeOH and LMeAl( $\mu$ -O)ZrRCp<sub>2</sub> (L = CH(N(Ar)(CMe))<sub>2</sub>, Ar = 2,6-*i*Pr<sub>2</sub>C<sub>6</sub>H<sub>3</sub>, R = Me, Cl) (1.961(3) Å).<sup>4</sup>

The Ti(1)–O(1) bond distance (1.808(3) Å) in compound **2** is significantly shorter when compared to those in [Cp<sub>2</sub>-Ti(CF<sub>3</sub>C=C(H)CF<sub>3</sub>)]<sub>2</sub>O (av Ti–O = 1.856(6) Å)<sup>24</sup> and the alkoxide bridged cluster (Ti<sub>4</sub>Zr<sub>2</sub>O<sub>4</sub>(OBU)<sub>n</sub>(OMC)<sub>10</sub> (OMC = methacrylate; n = 2, 4, 6; av Ti–O = 2.041(5) Å).<sup>25</sup> The Ti(1)–C(29) bond length (2.239(9) Å) is slightly longer when compared to those (av 2.175(5)) in Cp<sub>2</sub>TiMe<sub>2</sub>.<sup>26</sup>

The Ti–X<sub>Cp</sub> (X<sub>Cp</sub> = centroid of the Cp ring) distances in **2** are almost identical (av 2.108 Å) and are similar to those in dimethyltitanocene (av Ti–X<sub>Cp</sub> = 2.078 Å).<sup>26</sup> The X<sub>Cp1</sub>–Ti–X<sub>Cp2</sub> (X<sub>Cp</sub> = centroid of the Cp ring) bond angle (130.6°)

(20) Uhl, W.; Koch, M.; Hiller, W.; Heckel, M. *Angew. Chem.* **1995**, *107*, 1122–1124; *Angew. Chem., Int. Ed.* **1995**, *34*, 117–119.

(21) Kuhn, N.; Fuchs, S.; Niquet, E.; Richter, M.; Steimann, M. *Z. Anorg. Allg. Chem.* **2002**, *628*, 717–718.

(22) Hunter, W. E.; Hrcncir, D. C.; Vann Bynum, R.; Penttila, R. A.; Atwood, J. L. *Organometallics* **1983**, *2*, 750–755.

(23) Fronczek, F. R.; Baker, E. C.; Sharp, P. R.; Raymond, K. N.; Alt, H. G.; Rausch, M. D. *Inorg. Chem.* **1976**, *15*, 2284–2289.

(24) Rausch, M. D.; Sikora, D. J.; Hrcncir, D. C.; Hunter, W. E.; Atwood, J. L. *Inorg. Chem.* **1980**, *19*, 3817–3821.

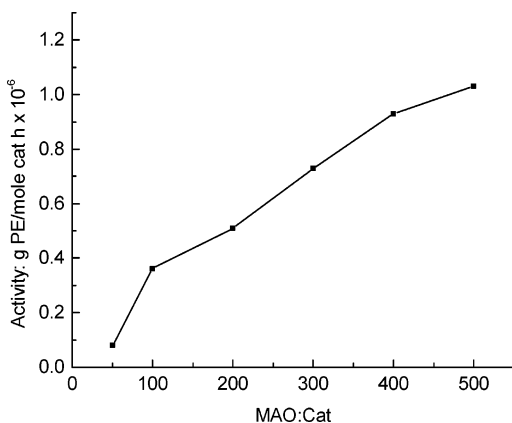
(25) Moraru, B.; Kickelbick, G.; Schubert, U. *Eur. J. Inorg. Chem.* **2001**, 1295–1301.

(26) Thewalt, U.; Wöhrle, T. *J. Organomet. Chem.* **1994**, *464*, C17–C19.

**Table 3.** Ethylene Polymerization Data for Compounds **2** and **3** as Catalysts<sup>a</sup>

catalyst	MAO/ catalyst	<i>t</i> (min)	PE (g)	activity ( $\times 10^6$ )	$M_w$	$M_w/M_n$
<b>2</b>	50	45	1.16	0.08	152817	6.01
<b>2</b>	100	30	3.5	0.36		
<b>2</b>	200	30	5.0	0.51		
<b>2</b>	300	17	4.0	0.73	97909	4.74
<b>2</b>	400	15	4.5	0.92	121996	4.57
<b>2</b>	500	15	5.0	1.03	106020	2.86
<b>3</b>	300	30	0.17	0.02		
<b>3</b>	400	30	0.43	0.04		
<b>3</b>	500	30	0.61	0.06		

<sup>a</sup> Polymerization conditions: for **2** and **3**, 19.5  $\mu$ mol, 100 mL of toluene at 25 °C, and 1 atm of ethylene pressure. Activity = g PE/mol cat h.

**Figure 3.** Plot of the activity toward the MAO/**2** ratios for ethylene polymerization.

in compound **2** is comparable to that in  $Cp_2TiMe_2$  ( $X_{Cp1}-Ti-X_{Cp2} = 134.5^\circ$ ).<sup>26</sup>

The Al-( $\mu$ -O) (1.71(2) Å) and Al-Me (1.965(2) Å) bond lengths in **3** are in the same range as those observed in **2**. The Hf(1)-O(1) (1.919(2) Å) and Hf(1)-C(7) bond lengths (2.281(2) Å) in **3** are shorter when compared to Hf-O (av 1.943 Å) and Hf-C (av 2.350 Å) in the homobimetallic compound ( $Cp_2RHf-(\mu-O)-HfRCp_2$ ) (R = Me,<sup>23</sup> Cl<sup>27</sup>). The Hf- $X_{Cp}$  (X = centroid of the Cp ring) distance in **3** (av 2.237 Å) is comparable to those of the homobimetallic ( $Cp_2-HfMe)_2(\mu-O)-Hf-X_{Cp}$  (av 2.210 Å).<sup>23</sup> The  $X_{Cp1}-Hf-X_{Cp2}$  (X = centroid of the Cp ring) bond angle (129.8°) in compound **3** is close to that in [ $(Cp_2HfMe)_2(\mu-O)$ ] (128.5°).<sup>23</sup>

**Ethylene Polymerization Studies.** The methylalumoxane (MAO)-activated compound of **2** exhibits high catalytic activity for the polymerization of ethylene, whereas the methylalumoxane (MAO)-activated compound of **3** shows low activity for the ethylene polymerization. All polymeric materials were isolated as white powders. Table 3 summarizes the polymerization results of catalysts **2** and **3**. Under comparable polymerization conditions, the MAO/**2** catalyst system shows almost similar activity to that of MAO/LMeAl-( $\mu$ -O)-Zr(Me)Cp<sub>2</sub> (L = CH(N(Ar)(CMe))<sub>2</sub>, Ar = 2,6-*i*Pr<sub>2</sub>C<sub>6</sub>H<sub>3</sub>).<sup>4</sup> Figure 3 exhibits the plot of activity for different ratios of MAO/**2** revealing a gradual increase in the activity with the MAO/**2** ratios. The data presented in

(27) Párkányi, L.; Sharma, S.; Cervantes-Lee, F.; Pannell, K. H. *Z. Kristallogr.* **1993**, *208*, 335–337.

**Table 4.** Styrene Polymerization Data for Compound **2** as Catalyst<sup>a</sup>

catalyst	MAO/ catalyst	<i>t</i> (min)	PS (g)	activity ( $\times 10^4$ )	$M_w$	$M_w/M_n$	$T_g^b$ (°C)
<b>2</b>	500	120	0.35	0.78			83.5
<b>2</b>	800	120	0.8	1.8	12989	7.46	76.5
<b>2</b>	1500	120	1.7	3.8			81.7

<sup>a</sup> Polymerization conditions: for **2**, 22.5  $\mu$ mol, 100 mL of toluene at 25 °C, and 10 mL styrene. Activity = g PE/mol cat h. <sup>b</sup> DSC.

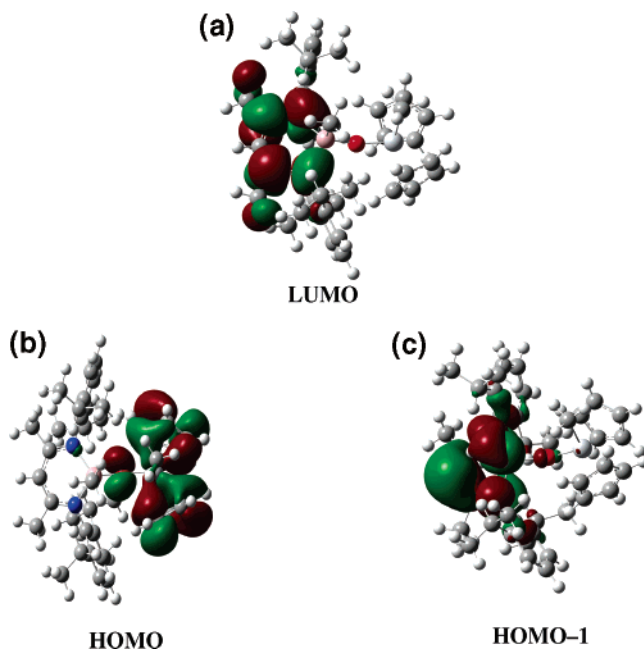
**Figure 4.** Computed frontier orbitals for the complex **2**: (a) LUMO, (b) HOMO, and (c) HOMO-1.

Table 3 clearly demonstrate that compound **2** acts as moderately active catalyst even at low MAO/**2** ratios; a similar result was previously observed for the corresponding Zr analogue of **2**.<sup>4</sup>

**Styrene Polymerization Studies.** The catalytic property of complex **2** for the polymerization of styrene was preliminarily investigated. This complex shows living catalyst activity at ambient temperature in toluene when activated with MAO. All polymeric materials were isolated as white powders, and Table 4 summarizes the activity values of catalyst **2**.

The DSC measurements of the polymers show that the characteristic glass-transition temperatures ( $T_g$ ) are in the range from 76 to 83 °C which is within the typical  $T_g$  range for the atactic polymers.<sup>28</sup> Melting points ( $T_m$ ) for the polymers were not observed. The GPC for measured polyethylene samples exhibit monomodal characteristics. The polydispersities show narrow distribution ranging from 2 to 6, which is typical for single-site catalysts.

**Results of Computational Studies.** To understand the catalytic process, we have carried out ab initio calculations for compound **2**. The frontier orbitals of complex **2** are shown in Figure 4. As can be directly seen from the orbital pictures, the HOMO and LUMO orbitals are located on different areas

(28) Guo, N.; Li, L.; Marks, T. J. *J. Am. Chem. Soc.* **2004**, *126*, 6542–6543.

**Table 5.** Selected Calculated and X-ray Bond Distances (Å) and Bond Angles (deg)

bond	calcd	X-ray	angles	calcd	X-ray
Al(1)–O(1)	1.749	1.715	O(1)–Al(1)–N(2)	114.02	113.90
Ti(1)–O(1)	1.840	1.808	O(1)–Al(1)–C(28)	115.36	115.20
Al(1)–C(28)	1.974	1.958	Al(1)–O(1)–Ti(1)	153.81	151.70
Ti(1)–C(29)	2.181	2.239	O(1)–Ti(1)–C(29)	95.59	95.60

of the molecule, and therefore, the metal centers Ti and Al show a completely different chemical behavior. As shown in Table 5, the resulting structure compares very well with the data obtained by X-ray crystallography, thus making it possible to obtain further insight into the molecular orbitals and bonds through analysis of the electronic structure.

The electronic stabilization of the metal cation formed during the activation by MAO is one of the key steps in the polymerization process. To address the factor which governs the stability of the cation, we studied the bonding situation in complex **2**. The NBO analysis<sup>16–18</sup> shows that the bond formed between the Ti atom and the oxygen (p-rich orbital on oxygen and pure d-orbital on titanium) obtains a significant stabilization of 26 kcal/mol through a donor acceptor interaction between the Ti(1)–O(1) bonding orbital with an unoccupied antibonding Al(1)–C(28) orbital. The combination of this stabilization with the lowest-unoccupied molecular orbital prevents bond breaking resulting from

changes of the electronic density on the Ti atom during the catalytic step.

In summary, we report the preparation, structural characterization, and catalytic property of two kinetically stable heterobimetallic complexes of Al(III) with Ti and Hf respectively binding through an oxygen bridge. Compound **2** exhibits high catalytic activity in ethylene and styrene homopolymerization. Computational study shows that the Ti cation center after activation by MAO is stabilized by the donor acceptor interaction between the Ti(1)–O(1) bonding orbital with an unoccupied antibonding Al(1)–C(28) orbital. Presently, we are studying the use of these compounds for copolymerization reactions.

**Acknowledgment.** This work is dedicated to Professor Karl Christe on the occasion of his 70th birthday. This work is supported by the Göttinger Akademie der Wissenschaften, Deutsche Forschungsgemeinschaft and the Fonds der Chemischen Industrie. S.K.M. thanks the Alexander von Humboldt Stiftung for a research fellowship. We thank the referees for their valuable suggestions.

**Supporting Information Available:** X-ray data (CIF) of **2** and **3**. This material is available free of charge via the Internet at <http://pubs.acs.org>.

IC060538R